

Article

# Matrix-Assisted Laser Desorption Ionization Mass Spectrometry of Compounds Containing Carboxyl Groups Using CdTe and CuO Nanoparticles

Megumi Sakurai <sup>1</sup>, Taro Sato <sup>2</sup>, Jiawei Xu <sup>2,3</sup>, Soichi Sato <sup>1</sup> and Tatsuya Fujino <sup>2,3,\*</sup>

<sup>1</sup> Department of Chemistry, Graduate School of Science and Engineering, Tokyo Metropolitan University, 1-1 Minami-Osawa, Hachioji, Tokyo 192-0379, Japan; sakurai-megumi@ed.tmu.ac.jp (M.S.); ssato@tmu.ac.jp (S.S.)

<sup>2</sup> Department of Applied Chemistry, Graduate School of Science and Engineering, Toyo University, 2100 Kujirai, Kawagoe 350-8585, Japan; s16d01400136@toyo.jp (T.S.); jiaweix0701@gmail.com (J.X.)

<sup>3</sup> Bio-Nano Electronics Research Centre, Toyo University, 2100 Kujirai, Kawagoe 350-8585, Japan

\* Correspondence: fujino048@toyo.jp; Tel.: +81-49-231-1481

Received: 14 February 2018; Accepted: 23 March 2018; Published: 26 March 2018



**Abstract:** Matrix-assisted laser desorption ionization mass spectrometry of compounds containing carboxyl groups was carried out by using semiconductor nanoparticles (CdTe and CuO) as the matrix. Salicylic acid (Sal), glucuronic acid (Glu), ibuprofen (Ibu), and tyrosine (Tyr) were ionized as deprotonated species (carboxylate anions) by using electrons ejected from CdTe after the photoexcitation. When CuO was used as the matrix, the peak intensity of Tyr became high compared with that obtained with CdTe. Measurements of model peptides, angiotensin II (AngII) and substance P (SubP), were also carried out but the obtained peak intensities were very low. In order to explain this result, the interaction between CdTe and AngII was confirmed by diffuse reflectance spectroscopy. The results suggest that electrostatic binding between semiconductor nanoparticles and AngII prevented the efficient desorption of AngII into the gas phase.

**Keywords:** MALDI; semiconductor; nanoparticles; carboxyl group

## 1. Introduction

Matrix-assisted laser desorption ionization mass spectrometry (MALDI MS) is a soft ionization method used to determine the molecular weight of an analyte. MALDI MS enables us to detect nonvolatile compounds, such as proteins and peptides, which are difficult to detect by other methods [1]. Some organic acids—such as  $\alpha$ -cyano-4-hydroxycinnamic acid (CHCA), sinapinic acid (SA), 2,5-dihydroxybenzoic acid (DHB), and 2,4,6-trihydroxyacetophenone (THAP)—are often used as the matrix. However, these organic matrices dissociate during the desorption/ionization process, thereby limiting the application of MALDI MS to low molecular weight compounds. In addition, the peak intensity of a protonated analyte is sometimes suppressed by an alkali metal ion adducted species. In order to overcome those drawbacks, several matrix-free techniques have been developed, including silicon nanowire (SiNW) [2], desorption/ionization on silicon (DIOS) [3,4], and nanostructure-initiator mass spectrometry (NiMS) [5]. The application of nanometer-sized particles—including Au [6], Ag [7], Pt [8], and Si [9]—instead of an organic matrix has also been proposed. In addition, the use of a co-matrix consisting of ammonium salt [9], phosphoric acid [10], serine [11], saccharide [12], and protein [13] with conventional organic matrix molecules is considered an effective way to improve the mass spectra as well.

Generally, it is known that fatty acids are difficult to ionize by MALDI MS using conventional organic matrix molecules. In our previous research, we revealed that CdTe nanoparticles ionized

fatty acids efficiently [14]. Electrons ejected from CdTe nanoparticles by Auger recombination after photoexcitation interacted with fatty acids to ionize them into carboxylate anion ( $\text{-RCOO}^-$ ) as  $\text{RCOO}^-$  was stabilized by resonance structures. In addition, CdTe nanoparticles were loaded on a zeolite surface to improve reproducibility of the peak intensity, and the complex of CdTe and zeolite was applied to the quantitative analysis of stearic acid in human serum.

Because it is understood that electrons ejected from CdTe nanoparticles react with carboxyl groups in fatty acids, we assumed that other compounds containing carboxyl groups could be ionized as well. In this study, CdTe was used to ionize such compounds as glucuronic acid (Glu), salicylic acid (Sal), ibuprofen (Ibu), tyrosine (Tyr), and model peptides, the structures of which contain carboxyl groups. As electrons ejected from a semiconductor are necessary for the ionization, we assumed that another semiconductor (CuO) would be also applicable to the ionization of the above-mentioned compounds. The purposes of this paper are to apply CdTe or CuO nanoparticles to the ionization of those molecules and to clarify the possible desorption and ionization mechanisms after the photoexcitation.

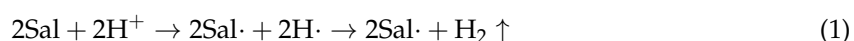
## 2. Materials and Methods

CdTe particles whose diameter was 250 nm (CdTe; 0.1 wt % water suspension without stabilizer) were purchased from Hamamatsu Nano Technology (Hamamatsu, Japan). Nanometer-sized CuO particles (<50 nm) were obtained from Sigma (Tokyo, Japan). Glu, Sal, Ibu, Tyr, and model peptides were purchased from Sigma.

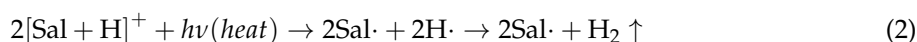
CdTe or CuO was used as the matrix. Those particles were dispersed in a mixture of acetonitrile and water ( $v/v = 7:3$ , 1 mL) and concentration was kept to 0.5 mg/mL or 4 mg/mL. An analyte was dissolved in another mixture of acetonitrile and water ( $v/v = 7:3$ ) and concentration was adjusted to 1 mg/mL. One microliter each of matrix and analyte solutions was pipetted onto a stainless steel plate and mixed several times to induce crystallization, and the solvent was evaporated in air prior to analysis by MALDI MS. Measurements were carried out with a time of flight (TOF) mass system (Waters) equipped with a nitrogen laser operating at 337 nm. The instrument was operated in the negative or positive ion mode and spectra were acquired with a reflectron. The laser power for excitation was 15  $\mu\text{J}$  except for measurements of a model peptide (21  $\mu\text{J}$  for substance P). Mass spectra were obtained by averaging 200 laser shots at random sample spots. Diffuse reflectance spectra were obtained by using an apparatus from Jasco (Tokyo, Japan) (V-650).

## 3. Results and Discussion

Figure 1a shows the laser desorption ionization (LDI) mass spectrum of Sal (sample only) in the negative ion region. The spectrum was obtained without use of any matrix. As Sal has an absorption coefficient at 337 nm, it was ionized to yield a deprotonated species,  $[\text{Sal} - \text{H}]^-$ , at  $m/z = 137$  even in the absence of a matrix. The LDI mass spectrum of Sal in the positive ion region is shown in Figure 1b. Although the S/N ratio was very low, peaks of radical cation species  $[\text{Sal}]^+$  and protonated Sal ( $[\text{Sal} + \text{H}]^+$ ) were observed at  $m/z = 138$  and 139.  $[\text{Sal} + \text{H}]^+$  and  $[\text{Sal} - \text{H}]^-$  were generated as a result of the dissociation of two Sal molecules in Sal crystals after the photoexcitation. As Sal is an acidic molecule, it could be easily deduced that proton adduction would be difficult and the peak intensity of  $[\text{Sal} + \text{H}]^+$  would be low. For the generation of the radical cation species,  $[\text{Sal}]^+$ , the following reaction would be expected.



Protons generated during the production of  $[\text{Sal} - \text{H}]^-$  species would attack Sal to remove an electron. Hydrogen radicals would terminate each other in the gas phase and a hydrogen molecule would be released. In addition, a reaction pathway using the hemolysis reaction would be also expected.



A proton-adducted species of Sal would be first generated by the adduction of a proton to one of the oxygen atoms in Sal, which would dissociate into two radical cation species using photon or heat energy.

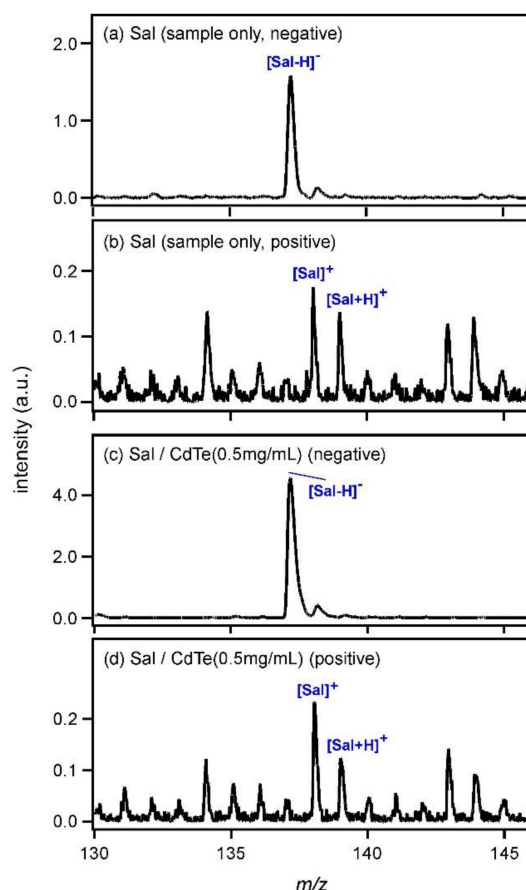
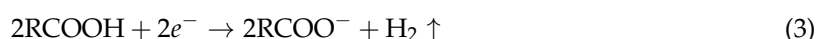


**Figure 1.** Laser desorption ionization mass spectrum of salicylic acid (Sal) in the (a) negative and (b) positive ion regions. Matrix-assisted laser desorption ionization mass spectrum of Sal with CdTe nanoparticles as the matrix (0.5 mg/mL) in the (c) negative and (d) positive ion regions.

Figure 1c shows the MALDI mass spectrum of Sal measured using CdTe nanoparticles (0.5 mg/mL) as the matrix. The peak intensity of [Sal-H]<sup>-</sup> increased; it was almost 2.9-fold higher than that in Figure 1a. In the positive ion region shown in Figure 1d, on the other hand, the peak intensities of [Sal]<sup>+</sup> and [Sal + H]<sup>+</sup> were almost equal to those in Figure 1b. This result clearly indicated that CdTe promoted the deprotonation of Sal. After the photoexcitation of CdTe, the following reaction would be expected.



Here, R represents the other groups of Sal. Electrons ejected from CdTe nanoparticles would react with the carboxyl groups of Sal and [Sal-H]<sup>-</sup> would be generated.

For other compounds containing carboxyl groups, MALDI MS was carried out using CdTe nanoparticles (0.5 mg/mL) as the matrix, and the obtained spectra in the negative ion mode are shown in Figure 2. The peak intensity of Glu ([Glu-H]<sup>-</sup>;  $m/z = 193.2$ ) shown in Figure 2a was increased compared with that obtained without CdTe (Figure 2b). In addition, the peak intensity of

Ibu ( $[\text{Ibu}-\text{H}]^-$ ;  $m/z = 205.3$ ) was slightly increased by using CdTe, as shown in Figure 2c,d. However, that of Tyr ( $[\text{Tyr}-\text{H}]^-$ ;  $m/z = 180.2$ ) almost disappeared when the CdTe matrix was used (Figure 2e,f). The pKa values were known as 2.9 for Sal, 3.2 for Glu, 4.5 for Ibu, and 2.2 for Tyr. As Tyr has the strongest acidity, the structure of the conjugate base must be the most stable among those four compounds. However, Tyr is an amino acid; it has an amino group as well as a carboxyl group. When a carboxylate anion was produced in a Tyr molecule according to Equation (3), it was expected that the amino group would catch a proton or an alkali metal cation to keep the molecular charge neutral. On the other hand, when Tyr crystals were photoexcited (Figure 2f), the same amounts of  $[\text{Tyr} + \text{H}]^+$  and  $[\text{Tyr}-\text{H}]^-$  ions were produced. Therefore, charge neutrality of the system was kept even after the photoexcitation and it was assumed that the buffer action of a Tyr molecule unlikely occurred, yielding a moderately intense peak (Figure 2f). Therefore, the concentration of the CdTe matrix was changed to 4 mg/mL in order to increase the number of electrons that could react with Tyr, and MALDI MS of Tyr was re-examined. The result is shown in Figure 2g. The peak intensity of  $[\text{Tyr}-\text{H}]^-$  was increased compared with that in Figure 2e, although the intensities of the other peaks were also increased. Therefore, it might be possible to consider that the deprotonation of Tyr was promoted as a large number of electrons that could overcome neutralization were generated from CdTe nanoparticles at 4 mg/mL.

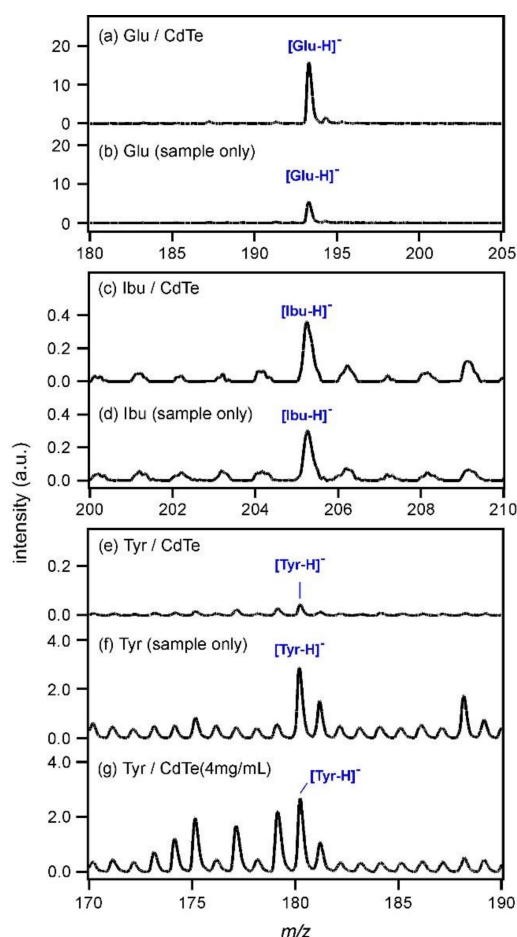


**Figure 2.** Mass spectra of glucuronic acid (Glu) (a) with CdTe nanoparticles as the matrix and (b) without matrix. Mass spectra of ibuprofen (Ibu) (c) with CdTe and (d) without matrix. Mass spectra of tyrosine (Tyr) (e) with CdTe, (f) without matrix, and (g) with CdTe (4 mg/mL).

From the above results, it was clarified that CdTe nanoparticles were applicable to the ionization of compounds containing carboxyl groups. The mechanism of electron ejection from CdTe in the

ionization of fatty acids was previously studied by us [14]. An electron ejected by Auger recombination after the photoexcitation reacted with a carboxyl group in fatty acids, and the deprotonation reaction was promoted. Auger recombination is not unique to CdTe; this process occurs in other semiconductors as well. Therefore, another semiconductor nanoparticle, CuO, was used for the measurement of Tyr and stearic acid (Ste). Figure 3a shows the mass spectrum of Tyr measured with CuO at the concentration of 4 mg/mL. The peak of  $[\text{Tyr-H}]^-$  was observed at  $m/z = 180$ . It was suggested that CuO had the same ability to deprotonate Tyr as CdTe by using an electron ejected after the photoexcitation. In addition, the peak intensity showed an almost 6.3-fold increase compared with that in Figure 2g. To understand the peak intensity change, a comparison of the zeta potential values of CuO and CdTe particles might be useful. It has been reported that the zeta potential usually changes with pH and that of CuO is approximately 25 mV around pH 7 [15–17] (sample preparation condition in this paper). CdTe nanoparticles used in this experiment were produced by laser ablation in water (without any stabilizer) and the CdTe nanoparticles easily aggregated in colloidal solution. Based on this fact, it was expected that the zeta potential of CdTe would be very small (approximately  $\pm 0$  mV). Therefore, the CuO surface was more positive than CdTe and it was assumed that CuO would attract lone-pair electrons from the oxygen or nitrogen atom in Tyr. Tyr could exist very near CuO so that electrons ejected from CuO would react with Tyr effectively, leading to the high peak intensity of  $[\text{Tyr-H}]^-$ . Then, Ste was subjected to MALDI MS using CuO nanoparticles. Figure 3b shows the mass spectrum of Ste; the peak of deprotonated Ste,  $[\text{Ste-H}]^-$ , was observed at  $m/z = 238$ . It was clarified that CuO had the ability to ionize fatty acids as well as CdTe. Measurements were also carried out for Ibu and Glu by using CuO, and spectra were shown in Figure A1 (Supplementary Materials).

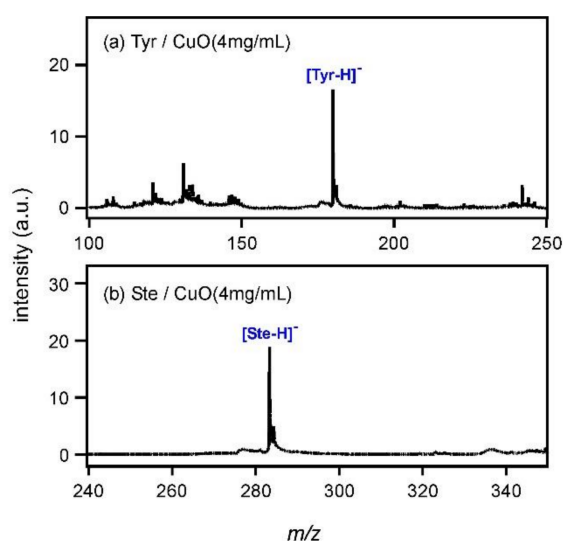


**Figure 3.** Mass spectra of (a) tyrosine (Tyr) and (b) stearic acid (Ste) with CuO nanoparticles as matrix (4 mg/mL).

As the next step, the ionization of a rather high molecular weight compound, angiotensin II (AngII), was examined by using CdTe nanoparticles (4 mg/mL). The mass spectrum is shown in Figure 4a. Although the peak intensity of deprotonated AngII ( $[\text{AngII-H}]^-$ ) was very low and many peaks originating in other species were observed, it was understood that CdTe could be a matrix for peptides as well. As the molecular weight of AngII is higher than those of the other compounds used in Figures 1–3, the number of AngII molecules is smaller as the concentration is the same (1 mg/mL). To explain the results in Figure 4, it was assumed that the distance between AngII and CdTe would be large, hindering efficient ionization. To confirm this assumption, AngII solution and CdTe dispersion were first mixed and then sonicated for 1 h to promote the mixing of those two compounds. The thus-obtained solution was subjected to MALDI MS and the spectrum is shown in Figure 4b. Contrary

to the above expectation, the peak of  $[\text{AngII}-\text{H}]^-$  could not be recognized clearly. Of course, it was possible that AngII was decomposed by the sonication. In fact, the intensities of the peaks around  $m/z = 220$  and  $863$  became twofold higher after the sonication (not shown), although those of the other peaks below  $m/z = 1000$  were almost unchanged. As another possibility, it was considered that AngII bound to CdTe strongly and the desorption of AngII to the gas phase was difficult. In a previous study of the interaction between CdS and hemoglobin, it was reported that electrostatic binding between those two molecules was induced [18]. Tellurium belongs to the same group as sulfur (S) on the periodic table. Although AngII does not have S in its structure, it has many oxygen (O) atoms and O belongs to the same group as S as well. Therefore, it might be possible to expect that electrostatic binding between AngII and CdTe was induced. The spectral feature observed in Figure 4 might also be explained by the HSAB (hard and soft acids and bases) theory. As CdTe is a semiconductor and charge density is expected to be approximately 0, CdTe is regarded as a soft acid. On the other hand, as AngII can easily polarize, AngII is regarded as a soft base. The soft acid CdTe and the soft base AngII attract each other and strong electrostatic binding between them is induced, making the desorption of AngII to the gas phase difficult.

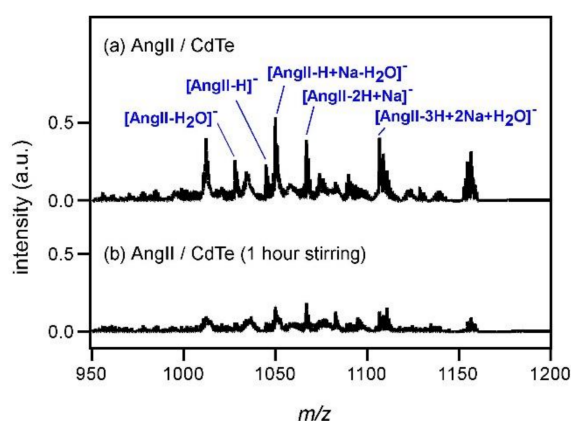
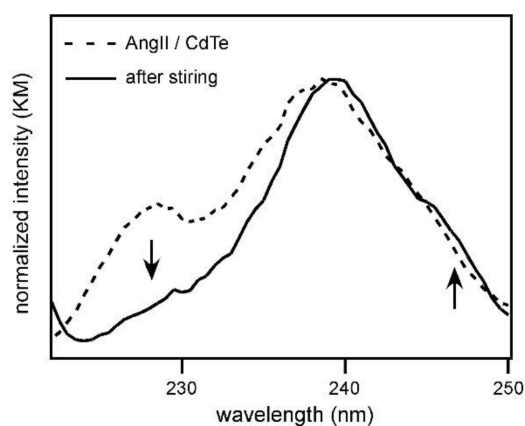


**Figure 4.** Mass spectra of angiotensin II (AngII) measured (a) with CdTe and (b) with CdTe after stirring for 1 h.

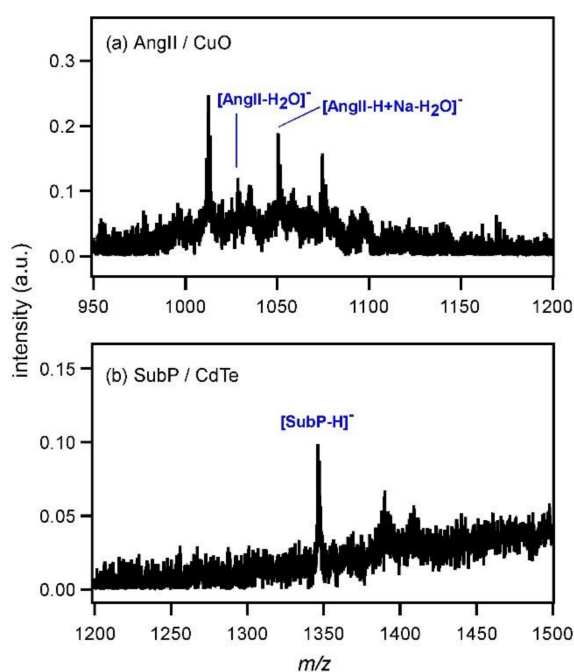
The above argument could be confirmed by measuring the diffuse reflectance spectra. Figure 5 shows the diffuse reflectance spectra of the mixed crystals of AngII and CdTe made in the same manner as that for MALDI MS measurements. The spectra obtained before and after stirring for 1 h are shown in the spectral region from 220 to 255 nm, and this region corresponds to the absorption by CdTe nanoparticles. After stirring for 1 h, the band around 225 to 230 nm decreased and a shoulder band newly appeared around 245 nm. In addition, the wavelength of the main peak, around 240 nm, was red-shifted by the stirring. These spectral changes clearly showed that CdTe interacted strongly with AngII and the energy of the electronic state of CdTe was changed. Therefore, it was verified that the strong electrostatic binding between CdTe and AngII prevented efficient desorption, and the peak intensity of AngII-related species became low.

Figure 6a shows the mass spectrum of AngII measured with CuO (4 mg/mL). The peak intensity was very low and the deprotonated peak of AngII was not observed. In addition, another peptide, substance P (SubP), was subjected to MALDI MS using CdTe as the matrix (0.5 mg/mL) (Figure 6b). The peak of  $[\text{SubP}-\text{H}]^-$  was observed at  $m/z = 1346$ ; however, its intensity was also very low. When the concentration of CdTe was increased to 4 mg/mL, the peak of  $[\text{SubP}-\text{H}]^-$  disappeared (not shown). By increasing the amount of CdTe, strong electrostatic binding occurred between CdTe and all SubP molecules so that the desorption of SubP was not possible anymore. The molecular weight of inorganic MALDI matrix, such as metal or semiconductor particles, is often higher than that of organic MALDI matrix. Therefore, metal or semiconductor particles hardly desorb to the gas phase and no

plume is produced after the photoexcitation. This aspect may be also unfavorable for the desorption of relatively heavy analytes, such as peptides.



**Figure 5.** Diffuse reflectance spectra of mixed crystals of angiotensin II (AngII) and CdTe before and after stirring for 1 h.



**Figure 6.** (a) Mass spectrum of angiotensin II (AngII) measured with CuO; (b) mass spectrum of substance P (SubP) measured with CdTe.

**Supplementary Materials:** The following are available online at <http://www.mdpi.com/2076-3417/8/4/492/s1>.

**Acknowledgments:** T.F. acknowledges a Grant-in-Aid for Scientific Research (B) (no. 15H03772) from JSPS.

**Author Contributions:** T.F. conceived and designed the experiments; M.S. and T.S. performed the experiments; M.S., J.X., and S.S. analyzed the data; M.S. contributed reagents/materials/analysis tools; T.F. wrote the paper.

**Conflicts of Interest:** The authors declare no conflict of interest.

## References

1. Tanaka, K.; Waki, H.; Ido, Y.; Akita, S.; Yoshida, Y.; Yoshida, T. Protein and polymer analyses up to  $m/z$  100,000 by laser ionization time-of-flight mass spectrometry. *Rapid Commun. Mass Spectrom.* **1988**, *2*, 151–153. [[CrossRef](#)]
2. Go, E.P.; Apon, J.V.; Luo, G.; Saghatelian, A.; Daniels, R.H.; Sahi, V.; Dubrow, R.; Cravatt, B.F.; Vertes, A.; Siuzdak, G. Desorption/Ionization on Silicon Nanowires. *Anal. Chem.* **2005**, *77*, 1641–1646. [[CrossRef](#)] [[PubMed](#)]
3. Trauger, S.A.; Go, E.P.; Shen, Z.; Apon, J.V.; Compton, B.J.; Bouvier, E.S.P.; Finn, M.G.; Siuzdak, G. High Sensitivity and Analyte Capture with Desorption/Ionization Mass Spectrometry on Silylated Porous Silicon. *Anal. Chem.* **2004**, *76*, 4484–4489. [[CrossRef](#)] [[PubMed](#)]
4. Wei, J.; Buriak, J.M.; Siuzdak, G. Desorption-ionization mass spectrometry on porous silicon. *Nature* **1999**, *399*, 243–246. [[CrossRef](#)] [[PubMed](#)]
5. Northen, T.R.; Yanes, O.; Northen, M.T.; Marrinucci, D.; Uritboonthai, W.; Apon, J.; Golledge, S.L.; Nordström, A.; Siuzdak, G. Clathrate nanostructures for mass spectrometry. *Nature* **2007**, *449*, 1033–1037. [[CrossRef](#)] [[PubMed](#)]
6. Huang, Y.-F.; Chang, H.-T. Nile Red-Adsorbed Gold Nanoparticle Matrixes for Determining Amino Thiols through Surface-Assisted Laser Desorption/Ionization Mass Spectrometry. *Anal. Chem.* **2006**, *78*, 1485–1493. [[CrossRef](#)] [[PubMed](#)]
7. Yang, M.; Fujino, T. Silver nanoparticles on zeolite surface for laser desorption/ionization mass spectrometry of low molecular weight compounds. *Chem. Phys. Lett.* **2013**, *576*, 61–64. [[CrossRef](#)]
8. Kawasaki, H.; Yonezawa, T.; Watanabe, T.; Arakawa, R. Platinum Nanoflowers for Surface-Assisted Laser Desorption/Ionization Mass Spectrometry of Biomolecules. *J. Phys. Chem. C* **2007**, *111*, 16278–16283. [[CrossRef](#)]
9. Wen, X.; Dagan, S.; Wysocki, V.H. Small-Molecule Analysis with Silicon-Nanoparticle-Assisted Laser Desorption/Ionization Mass Spectrometry. *Anal. Chem.* **2007**, *79*, 434–444. [[CrossRef](#)] [[PubMed](#)]
10. Kjellstro, S.; Jensen, O.N. Phosphoric Acid as a Matrix Additive for MALDI MS Analysis of Phosphopeptides and Phosphoproteins. *Anal. Chem.* **2004**, *76*, 5109–5117. [[CrossRef](#)] [[PubMed](#)]
11. Nishikaze, T.; Takayama, M. Disappearance of interfering alkali-metal adducted peaks from matrix-assisted laser desorption/ionization mass spectra of peptides with serine addition to  $\alpha$ -cyano-4-hydroxycinnamic acid matrix. *Rapid Commun. Mass Spectrom.* **2007**, *21*, 3345–3351. [[CrossRef](#)] [[PubMed](#)]
12. Koster, C.; Castoro, J.A.; Wilkins, C.L. High-Resolution Matrix-Assisted Laser Desorption/Ionization of Biomolecules by Fourier Transform Mass Spectrometry. *J. Am. Chem. Soc.* **1992**, *114*, 7572–7574. [[CrossRef](#)]
13. Kobayashi, T.; Kawai, H.; Suzuki, T.; Kawanishi, T.; Hayakawa, T. Improved sensitivity for insulin in matrix-assisted laser desorption/ionization time-of-flight mass spectrometry by premixing  $\alpha$ -cyano-4-hydroxycinnamic acid matrix with transferrin. *Rapid Commun. Mass Spectrom.* **2004**, *18*, 1156–1160. [[CrossRef](#)] [[PubMed](#)]
14. Yang, M.; Fujino, T. Quantitative analysis of free fatty acids in human serum using biexciton Auger recombination in cadmium telluride nanoparticles loaded on zeolite. *Anal. Chem.* **2014**, *86*, 9563–9569. [[CrossRef](#)] [[PubMed](#)]
15. Chang, H.; Jwo, C.S.; Lo, C.H.; Tsung, T.T.; Kao, M.J.; Lin, H.M. Rheology of CuO nanoparticle suspension prepared by ANSS. *Rev. Adv. Mater. Sci.* **2005**, *10*, 128–132.
16. Li, C.-C.; Chang, M.-H. Colloidal stability of CuO nanoparticles in alkanes via oleate modifications. *Mater. Lett.* **2004**, *58*, 3903–3907. [[CrossRef](#)]
17. El-Trass, A.; ElShamy, H.; El-Mehasseb, I.; El-Kemary, M. CuO nanoparticles: Synthesis, characterization, optical properties and interaction with amino acids. *Appl. Surf. Sci.* **2012**, *258*, 2997–3001. [[CrossRef](#)]
18. Shen, X.-C.; Liou, X.-Y.; Ye, L.-P.; Liang, H.; Wang, Z.-Y. Spectroscopic studies on the interaction between human hemoglobin and CdS quantum dots. *J. Colloid Interface Sci.* **2007**, *311*, 400–406. [[CrossRef](#)] [[PubMed](#)]

